PERGAMON

Vision Research 38 (1998) 2099–2108

Vision Research

Motion blur and motion sharpening: temporal smear and local contrast non-linearity

Stephen T. Hammett [a,*], Mark A. Georgeson [b], Andrei Gorea [c]

[a] *Department of Psychology, University of Glasgow, 62 Hillhead Street, Glasgow G12 8QQ, UK*
[b] *School of Psychology, University of Birmingham, Birmingham B15 2TT, UK*
[c] *Laboratoire de Psychologie Expèrimentale, CNRS & Université René Descartes (Paris V), 28 rue Serpente, 75006, Paris, France*

Received 29 May 1997; received in revised form 12 November 1997

Abstract

Blurred images may appear sharper when drifting than when stationary. But, paradoxically, moving sharp edges may appear more blurred. To resolve this paradox, the perceived sharpness of drifting, blurred, square wave gratings was compared with that of their static analogues over a range of speeds, blurs and spatial frequencies. Both motion blur and motion sharpening occurred, depending upon the physical blur of the patterns. For large extents of blur (>10 min arc) moving patterns always appeared sharper than their static analogues, but for small blurs (<10 min arc) moving edges appeared more blurred than stationary ones. We present a quantitative model for the distortion of waveforms in motion based on two factors: (i) visual temporal integration that smears moving images, and (ii) a local contrast non-linearity that increasingly sharpens the effective profile of edges as speed and contrast increase. We suggest that a plausible account of the speed-dependent non-linearity is the differential recruitment of M and P cells at different speeds.

Keywords: Motion; Perceived blur; Contrast; Speed; Non-linearity; Temporal filtering; M and P cells

1. Introduction

Estimates of the integration time of the human visual system range from relatively short durations of around 35 ms [1,2] to around 120 ms [3,4]. The existence of a finite integration period, regardless of its precise duration, leads to the prediction that objects in motion should appear more blurred than their static analogues since their position changes during the integration period. The duration of the integration period will determine the degree of perceived blur at a particular speed. Indeed, studies of perceived blur [5] and blur discrimination ([6] but see also ref. [7]) indicate that motion does increase perceived blur under certain conditions. However, the extent of perceived blur is less than would be expected from the larger estimates of integration time [8]. From these findings, several models of motion deblurring have been proposed [9–11]. Whilst these models differ in detail, they all propose that the visual system compensates for or removes blur introduced by motion. It is worth noting that the evidence for any such deblurring mechanism relies on the assumption that the integration period of the system is around 120 ms, rather than the shorter estimates around 35 ms.

Paradoxically, several recent reports [12,13] have confirmed the observation of Ramachandran et al. [14] that blurred images appear sharper when moving. Whilst motion deblurring would preserve the sharpness of moving objects that should otherwise appear blurred, most models of deblurring do not predict sharpening of moving blurred objects (although see ref. [15]). Hammett and Bex [13] measured the effect of adapting to a missing-fundamental (MF) pattern on perceived sharpness of drifting sinusoidal patterns. The MF pattern is a square wave grating with the fundamental frequency component (f) removed. It contains higher spatial frequencies at the odd harmonics ($3f$, $5f$, $7f$,...).Hammett and Bex [13] found that the degree of motion sharpening at test frequency f was smaller after adaptation to MF patterns, and proposed that motion sharpening may be due to an early non-lin-

* Corresponding author. Tel.: +44 141 3303612; fax: +44 141 3398889x; e-mail: shammett@psy.gla.ac.uk.

0042-6989/98/$19.00
PII: S0042-6989(97)00430-6

earity which introduces higher spatial frequencies into the effective neural image. These distortion products would be attenuated by adaptation to the MF pattern.

To summarise, previous findings have shown that sharp images undergo blurring in motion whilst blurred images appear sharper in motion. What determines whether a particular waveform undergoes sharpening or blurring, and what is the relationship between the two phenomena? In order to clarify the nature of motion sharpening and motion blur, we measured the perceived blur of a number of drifting waveforms as a function of speed, blur and spatial frequency. The results are considered with respect to both periodicity and local profile and we present a model which accounts for motion blurring and sharpening via a two stage process: (i) linear temporal filtering and (ii) non-linear, speed dependent local contrast encoding.

2. Methods

2.1. Apparatus and stimuli

Stimuli were generated by a VSG2/3W (Cambridge Research Systems) graphics generator with 14 bit resolution. Stimuli were displayed on a NEC XP17 colour display at a frame rate of 119 Hz. The mean luminance was 31 cd m^{-2}. The display was gamma corrected using internal look-up tables. The stimuli were displayed in two windows, equidistant from a central dark fixation point. The windows subtended 6° × 3° (vertical × horizontal) and were separated horizontally by 1°. The viewing distance was 114 cm.

The stimuli were horizontal periodic patterns whose luminance profile was manipulated such that the hard edges of a square wave were replaced by half a cycle of a sine-wave centred on the edges (see Fig. 1 and ref. [12]). In the limiting cases, the pattern was either a sinusoid (defined as 100% blur) or a square wave (defined as 0% blur). Intermediate blur widths were produced by replacing the edges of the square wave by sinusoidal profiles centred on the edge (see Fig. 1). Blur width is given by the half-period (h) of this sinusoidal profile. Blur (as % of maximum achievable blur) is defined as $100[2hf]$ where f is fundamental spatial frequency. The patterns were either stationary or drifted vertically at a range of speeds. The spatial frequencies of the patterns were nominally at octave intervals 0.25, 0.5, 1, 2 cd —exact values used to calculate blur widths were 0.27, 0.47, 1.01 or 2.02 cd —and Michelson contrast (m) was 0.3.

2.2. Procedure

Standard and test patterns of the same spatial frequency were presented simultaneously in the two windows, and the left or right position of the two patterns was randomised from trial to trial. The patterns were presented for 500 ms with abrupt onset and offset[1]. Between presentations, a homogeneous grey field of mean luminance was presented. The spatial phase of the standard and test patterns was randomised from presentation to presentation. The standard pattern was a drifting blurred square wave whose blur width was constant in any session (15, 25, 50 or 100%). At the beginning of each session the blur profile of the stationary test pattern was randomised such that it was between 5 and 20% sharper than that of the standard pattern. The blur width of the test pattern subsequently varied from trial to trial depending upon the subject's previous responses. Its blur width was determined by a modified Pest procedure [16] set to converge on the 50% point. The subjects' task was to indicate which of the two patterns appeared sharper by pressing a button. The standard and test were always of the same spatial frequency. The test pattern was static and the standard pattern drifted vertically at 2, 4, 8, or 16°s^{-1}. The direction of motion of the standard pattern (up or down) was randomised from trial to trial. In any particular session only one spatial frequency and one test speed were presented. Each session consisted of 50 trials for each speed. The 50% point of the resultant psychometric function was estimated by Probit analysis. The PSE was taken to be the mean of three such estimates. The order of sessions was pseudo-random.

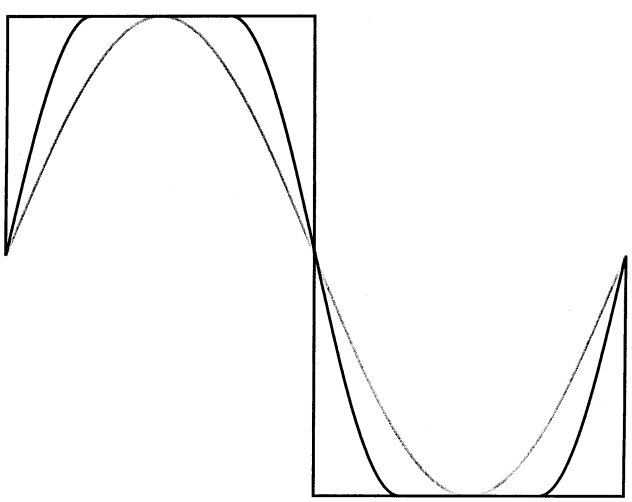

Fig. 1. The figure illustrates the change in luminance profile of stimuli from square-wave to sinusoid, defined as 0 and 100% blurred respectively. The grey lines represent intermediate blur profiles, constructed by replacing the square-wave edges with half-sines centred on the edges.

[1] Pilot experiments revealed that the task was considerably easier at this relatively long presentation duration than at shorter durations. In order to ensure that pursuit eye movements had not confounded our results we conducted auxilliary experiments at a presentation duration of 125 ms. The results yielded no quantitative difference, but an increase in the S.E.M. which presumably reflected the greater task difficulty.

Two subjects participated in the experiment, one of the authors (S.T.H.) and a naive observer (S.B.). Viewing was binocular and no head restraint was used. The experiment was conducted in a semi-darkened room.

3. Results

Fig. 2 plots the ratio of the matching blur width to standard blur width as a function of speed for 15, 25, 50 and 100% blur conditions. Values of this ratio below 1.0 represent a perceptual sharpening of the moving pattern relative to the static analogue whereas values above 1.0 represent a perceptual blurring of the moving pattern. At 100% blur, i.e. with sinusoidal standard gratings, all spatial frequencies tested yielded match ratios below 1.0. There was a small but consistent trend for perceived sharpness to increase monotonically with speed for all speeds tested, consistent with previous findings [12]. For patterns of 50% blur, all but the highest spatial frequency tested (2 cd) yielded similar results. However, at 2 cd, matches at $4°s^{-1}$ were above 1.0 and represent a perceptual blurring of the pattern. For conditions where the patterns are blurred by 25% of the maximum achievable blur, this progressive blurring of patterns with increasing speed extends to patterns of 1 cd and for the sharpest standard patterns employed (15% blur) all patterns except the lowest spatial frequency (0.25 cd) yielded perceptual blur which increased monotonically with speed. Thus whilst moving sinusoidal patterns appeared sharper than their static analogues, sharper patterns tended to appear more blurred. Both motion sharpening and blurring occurred for all but the lowest spatial frequency.

Spatial frequency is not the critical factor determining whether motion produces greater apparent sharpness or greater blur. This is clearly indicated in Fig. 5, where at small blur widths ($<10'$), motion always led to an increase in perceived blur, regardless of spatial frequency or speed. Conversely, at larger blur widths ($>10'$) motion always yielded a perceptual sharpening of the pattern. The critical factor determining the occurrence of blur or sharpening appears to be standard blur width rather than periodicity. We next present a model of how both blur and sharpening may depend upon blur width and yet be independent of the periodicity of the pattern.

4. Motion sharpening: a model based on local contrast transducers

4.1. Defining the stimulus.

At any one instant the moving stimulus has a spatial waveform $I(x)$ that can be defined by:

$$I(x) = L_0[1 + m \cdot f(x)] \tag{1}$$

where $f(x)$ is a function with unit amplitude (i.e. range $[-1, 1]$), and m is the Michelson contrast of the image ($0 \le m \le 1$). The local contrast function $C(x)$ is defined as:

$$C(x) = \frac{I(x) - L_0}{L_0} = m \cdot f(x) \tag{2}$$

4.2. Defining the transducer

The output $r(x)$ of the transducer, given the input $C(x)$, is defined by a version of the Naka-Rushton equation:

$$r(x) = r_{\max} \cdot \frac{C(x)}{|C(x)| + S} \tag{3}$$

where S is the semi-saturation contrast, at which $r(x) = r_{\max}/2$. Note that $r_{\max}$ is the theoretical maximum value of the function (as $C \to \infty$) not the value attained when $C = 1$. This transducer applies a similar compressive transformation to both positive and negative values of local contrast, and preserves the sign of the input signal. The transducer is highly compressive when S is small and tends to linearity when S is large. We assume in this paper that perceived blur depends upon the shape of the response profile, and so without loss of generality we can let $r_{\max} = 1$. This amounts to saying that the units of response measurement are arbitrary. It follows from Eqs. (2) and (3) that

$$r(x) = \frac{(m/S) \cdot f(x)}{(m/S) \cdot |f(x)| + 1} \tag{4}$$

Thus for a given waveform $f(x)$ the output depends only on the ratio (m/S). This is a useful simplification, and shows that the distortion of $f(x)$ will depend upon stimulus contrast relative to the compressiveness of the transducer.

4.3. The blur look-up table

Our aim is to find out the extent to which the transducer alters the profile, and hence blur, of an input waveform. One way to do this would be to define a model for blur encoding, and then determine how the blur code is altered by the transducer. One such blur code is based on the ratio of first to third spatial derivatives of the spatial waveform [17]. But it proved impossible to derive a tractable analytic expression for the blur of the transduced waveform, and in any case we might prefer to derive results that do not depend upon a particular model of blur encoding. We therefore adopted a computational approach by fitting a suitable ogive [the logistic function, whose form when scaled to the range $(-1, 1)$ is $y = 2/(1 + \exp(-x/s)) - 1]$ to

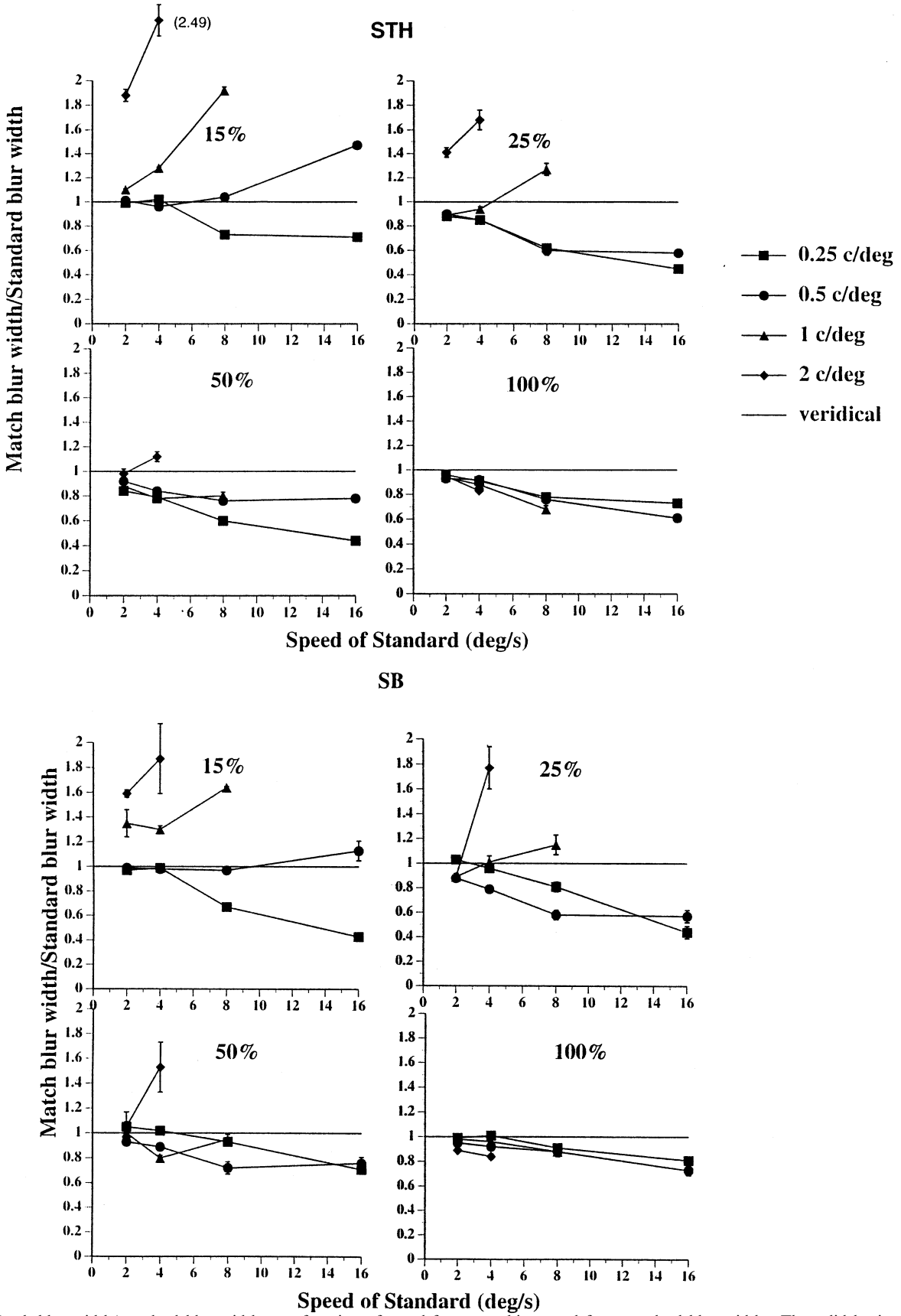

Fig. 2. Match blur width/standard blur width as a function of speed for two subjects and four standard blur widths. The solid horizontal line represents veridical matches. Values above 1 indicate the introduction of perceived blurring and values below 1 represent sharpening. Error bars represent ± 1 S.E.M.

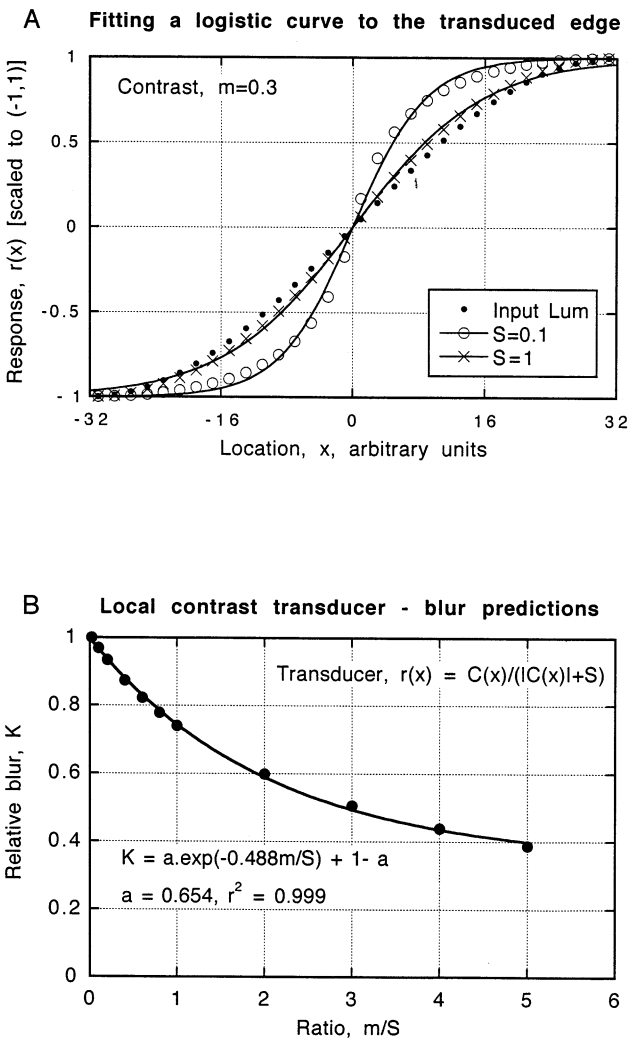

Fig. 3. How the contrast transducer affects edge blur. (A) Filled symbols show samples of a sine-wave luminance edge profile; other points show the response $r(x)$ of the model's contrast transducer, for two values of the parameter S (0.1, 1). Input contrast was 0.3, as in the experiments. Both input and output have been scaled to the range $[-1, 1]$ for this plot. Note how the most compressive transducer ($S = 0.1$) sharpens the waveform. Smooth curves show the best-fitting logistic functions used to quantify the change in blur. (B) The proportional change in blur (K) depends only on the ratio m/S, as shown. The fitted exponential function was used to generate blur-matching predictions for different values of m and S.

$r(x)$, and simply assuming that the scale parameter (s) is proportional to encoded blur. For the matching experiments this amounts to assuming that two waveforms will appear to match in blur when their fitted ogives have the same profile shape (determined by scale, s). Fig. 3(A) illustrates this process, showing that for a transducer with $S = 1$ there is little distortion of the input waveform, but with $S = 0.1$ the waveform is considerably sharpened. The proportional change (K) in blur produced by each value of (m/S) is defined as $K = s/s_0$, where s_0 is the scale of the undistorted input waveform. In the examples of Fig. 3(A), with $m = 0.3$, $K = 0.90$ when $S = 1$ but $K = 0.50$ when $S = 0.1$. The values of K were tabulated for many values of (m/S), and as Fig. 3(B) shows, they were well fitted by the following exponential function, which was then used in all subsequent modelling and data-fitting:

$$K = a \cdot \exp(-0.488 m/S) + b \quad (5)$$

where $a = 0.6538$, $b = (1 - a)$. Note that there are really no free parameters in Eq. (5). Its form and the values of a and b are determined directly by the form of the transducer $[C/(|C| + S)]$ adopted in Eq. (3). Note also that $K \leq 1$, meaning that this transducer predicts a sharpening of the input waveform (less blur) with increasing values of (m/S).

4.4. Empirical relation between transducer (S) and speed (V)

For input blur values of 15 min or more, our data and those of Bex et al. [12] show a progressive decrease of perceived blur with increasing speed. Both data sets could be fairly well described by the simple assumption that the semi-saturation contrast is inversely proportional to speed:

$$S = \frac{\alpha}{V} \quad (6)$$

That is, the local contrast transducer is more compressive at higher speeds. Later in the paper we develop the argument that this is related to differences in the contrast response functions of P and M cells. Combining Eqs. (5) and (6) we get:

$$K = a \cdot \exp(-0.488 m \cdot V/\alpha) + b \quad (7)$$

From this we derive the prediction that the sharpening factor (K) should depend on both contrast (m) and speed (V) in the same way. In fact, the sharpening effect should depend only on the product (mV) of contrast and speed. Fig. 4 shows data from two experiments by Bex et al. [12] that confirm this prediction. In one experiment (filled symbols) 5 contrast levels (10–50%) were tested at two speeds (1.8, 7.2°s^{-1}) and in the other experiment (open symbols) 3 contrast levels (10, 30, 50%) were tested at four speeds (1.8–7.2°s^{-1}). Apart from one or two wayward points (arising from one subject in one experiment), the bulk of the blur-matching data (means of two observers) fall close to a single decreasing function of $m.V$. The solid curve shows that Eq. (7) fits the main trend of the data very well when $\alpha = 1.44$[2].

[2] The curve actually shows the function $B.K$ where B is the baseline match made when $V = 0$, and K is the sharpening factor as discussed. We should expect $B = 30$ min arc, since that was the actual blur of the stimuli; Bex et al, however, did not measure B, and inspection of the data (Fig. 4) suggests that the data converge to a value rather less than 30 min. It turned out that $B = 28.5$ min gave a better fit than $B = 30$. This suggests the presence of a small constant error in their matching task.

4.5. Motion blur and motion sharpening combined

The distorting effect of the transducer accounts for motion sharpening, but not for the motion blur observed when input blur was small. We assume quite conventionally that linear, low-pass temporal filtering (motion smear) accounts for this effect. These two influences on blur can be readily linked into one model as follows. We assume that the linear filtering occurs (e.g. in the photoreceptors) before the contrast transducer (e.g. in the ganglion cells). Let h_B be the standard blur (half-period, min arc) and h_V be the motion blur induced at speed V. Since variances add under convolution [18] we can see that the waveform input to the transducer will have a blur equal to $\sqrt{h_B^2 + h_V^2}$. The transducer modifies this blur by a factor K, described above Eqs. (5)–(7). The effective blur h_E at the transducer output is therefore:

$$h_E = K\sqrt{h_B^2 + h_V^2} \tag{8}$$

We can also usefully translate the spatial smear (h_V) induced by motion into the temporal extent of the filter's impulse response. Georgeson [17] showed that both theoretically and experimentally a sine-wave edge (as used here) with half-period h was equivalent in blur to a Gaussian-blurred step-edge, where the Gaussian had a standard deviation σ, such that $\sigma = h/\pi$. Suppose that the low-pass temporal filter's impulse response can also be described by a Gaussian function of time, with S.D. σ_t. At speed V, a response of duration δt would be smeared over a distance $\delta x = V\delta t$. Hence the spatial equivalent blur $\sigma_V = V\sigma_t$, and since $h = \sigma\pi$:

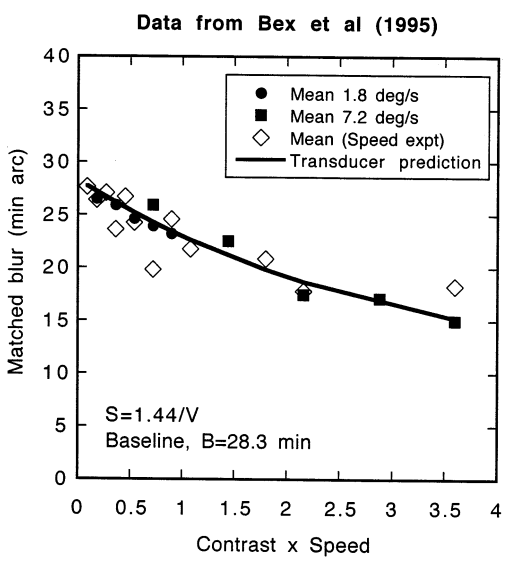

Fig. 4. Blur-matching data from experiments 1 and 2 of Bex et. al. [12], compared with predictions from the contrast transducer. Each data point is the mean of the two observers tested. Curve shows the decrease in blur predicted by the assumption that the transducer parameter S varies inversely with speed, V. Abscissa is the product of contrast (range 0.1–0.5) and speed (range 1.8–7.2°s^{-1}).

$$h_V = \sigma_t \cdot V \cdot \pi \tag{9}$$

Collecting all these arguments together (Eqs. (5) and (9)), we arrive at a single expression that defines the effective spatial blur of moving edges:

$$h_E = \{1 + 0.6538 \cdot [\exp(-0.488 m V/\alpha) - 1]\} \times \sqrt{h_B^2 + (\sigma_t \cdot V \cdot \pi)^2} \tag{10}$$

This expression defines the model to be applied to the present data. It has 3 stimulus variables (m, V, h_B) and two free parameters (α, σ_t). Note that for a stationary edge ($V = 0$), $h_E = h_B$; the transducer is linear and motion smear is absent. In our matching experiments the comparison stimulus was stationary. Hence, to predict blur-matching results we assume that an observer matches the equivalent blurs of the moving and stationary patterns, from which it follows that Eq. (10) should represent the physical blur of a stationary stimulus that is required to match the perceived blur of a moving one.

4.6. Fitting the results

Best-fitting values of (α, σ_t) were derived for the two observers (SH, SB) separately, using the error minimization routine ('Solver') in Microsoft Excel 4.0, where the error measure was the sum of the squared differences between predicted and observed log blur across the whole data set. The use of log blur is preferred (a) because the discriminability of blur, and therefore the reliability of different blur matches, is approximately equal on a log blur scale, and (b) because the log scale gives equal weight to proportional changes in blur at large and small values. This allows both the motion sharpening and motion blur effects to contribute substantially to the overall fit of the model.

Fig. 5 shows that the model describes very well the data of SH and SB, capturing both the sharpening effect of speed at large blurs, and the blurring effect at small blurs. Both model and data show a balance of these two effects around 10 min arc blur. The best-fitting parameter values for these data were $\alpha = 1.59$, $\sigma_t = 7.7$ ms (SH) and $\alpha = 2.55$, $\sigma_t = 5.1$ ms (SB). If we take 'integration time' to be the Gaussian equivalent width of the impulse response ($2.5\sigma_t$), then the duration of temporal integration responsible for motion smear in these experiments was around 13–19 ms. These estimates are in good agreement with those of Pääkönen and Morgan [6] who reported S.D. of the temporal impulse response to fall within the range of 4–6 ms. Furthermore, their analysis indicates that their estimates (and thus the present estimates) are consistent with previous comparable studies of integration time in motion [19,20]. What degree of spatial blur (σ_V) is implied by this temporal smear? From Eq. (9) we get $\sigma_V = V\sigma_t$ and so taking $\sigma_t = 6.4$ ms (mean of the two

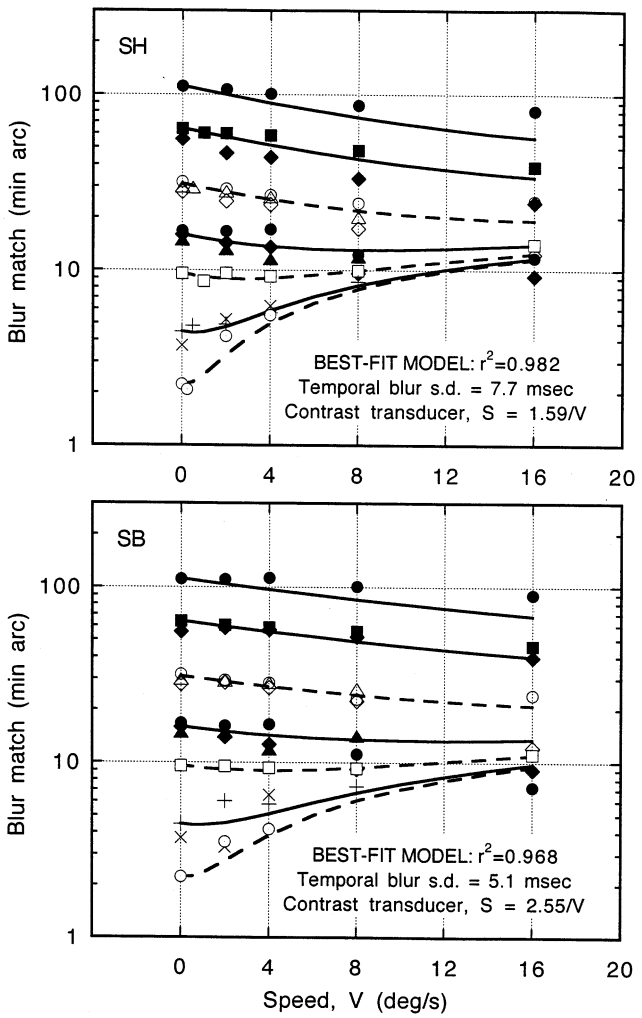

Fig. 5. Blur matching as a function of speed, for two observers. Symbols at $V = 0$ represent the actual blur (h, min arc) of the moving standard edge. From the top, the standard blur widths (and nominal spatial frequencies-see Section 2) were: filled circle: 112′ (0.25 cd); filled square: 64′ (0.5); filled diamond: 56′ (0.25); open circle: 32′ (0.5); open triangle: 30′ (1.0); open diamond: 28′ (0.25); filled circle: 16.7′ (0.25), filled diamond: 16′ (0.5); filled triangle: 14.9′ (1.0); open square: 9.6′ (0.5); plus (+): 4.5′ (1.0); cross (x): 3.7′ (2.0); open circle with dot: 2.2′ (2.0). Curves show the values produced by the best-fitting predictions of the model at each of seven standard blurs: 112, 64, 31, 16, 9.6, 4.5, 2.2 min arc.

observers) we find that at $V = 1°s^{-1}$ σ_V is small (0.4 min arc) while at $16°s^{-1}$ it is substantial (6.1 min arc).

Fig. 6 shows the same model (Eq. (10)) fitted to data of Bex et al. [12] as a function of contrast at two speeds (again taking the baseline match to be 28.5 min). The best-fitting value of σ_t was 9.5 ms. This is surprisingly close to the value obtained from our own data, given that the Bex data were collected only at a large blur (30 min) where the effect of temporal smear is counteracted by the sharpening effect. Interestingly, the effect of motion smear in the model predicts that, at low contrasts, blur matches for high-speed should rise above those for low speed. Though the data do not extend to contrasts low enough to show this, they do converge nicely around 10% contrast in a way consistent with the predicted cross-over. The inclusion of temporal smear in the model necessarily modifies the estimate of α, compared with the case where predictions were derived from the transducer alone (Fig. 4). For the Bex data the value of α fell from 1.44 without temporal smear to 1.14 with the inclusion of temporal smear.

5. Discussion

The empirical results reported here clearly indicate that waveforms in motion may undergo sharpening or blurring. Consistent with previous reports [12–14] moving blurred waveforms appeared sharper than their static analogues. Conversely, relatively sharp patterns appeared more blurred when moving. The effects of both motion sharpening and motion blur increase with speed. All but the lowest spatial frequency suffered both sharpening and blurring, depending upon the sharpness of the profile used. Thus the periodicity of the pattern does not appear to be a critical factor. Rather, the critical factor appears to be the physical blur width of the edges (Fig. 5). Small blur widths ($< 10'$) always gave motion blur (indicated by a positive slope), regardless of spatial frequency or speed, whereas larger blur widths ($> 10'$) always gave motion sharpening (a negative slope). The model we have presented successfully characterises these findings by assuming (i) that the finite integration time of the system smears the moving image and (ii) that the local contrast-response function becomes progressively more compressive as speed increases. The magnitude of motion blur depends on speed but is independent of stimulus blur; hence it is a relatively large effect only for small input blurs (Eq. (8)). Conversely, motion sharpening (in the model) depends on contrast and speed, but scales up with stimulus blur. The two effects balance around 10 min arc blur, but sharpening increasingly outweighs motion blur at higher levels of stimulus blur. The model fits are in good agreement with our results across all conditions and also fit well the data from experiments 1 and 2 of Bex et. al. [12] at different contrasts and speeds (Fig. 6). [A referee pointed out that experiment 3 of Bex et. al. [12] did not appear to show a systematic effect of contrast. The contrasts used there were 30 and 50%, and a glance at Fig. 6 here reveals that only small differences in blur are expected between 0.3 and 0.5 contrast. These small differences could easily be hidden by noise in the data. The data of Hammett and Bex [13] are not directly relevant to the present model, since they measured blur discrimination, not blur matching.]

The model has two main features. Firstly we propose an early linear temporal filter which smears edges in motion. Pääkönen and Morgan [6] reported evidence from the results of dynamic blur discrimination thresholds that the impulse response of this mechanism has a S.D. of around 4–6 ms, and in a meta-analysis of other results they estimated values of 5.8–9.5 ms, in good agreement with the present estimates of 7.7 ms for subject STH and 5.1 ms for subject SB. Taking the width of the impulse response as $2.5\sigma_t$ yields estimates of motion integration time between 13 and 19 ms for our data. Pääkönen and Morgan took integration time to be the full width of the positive lobe of the temporal impulse response, and estimated this to be around 25 ms. This higher value arises merely from a different definition of 'width'. The important point is that estimates of σ_t (and hence integration time) are in relatively good agreement across a wide range of studies.

The second feature of our model is the velocity dependence of the semi-saturation constant in local contrast encoding. A physiological basis for this could be the differential recruitment of M and P cells with speed. Kaplan et. al. [21] fitted Eq. (3) to the averaged responses of a group of 8 M-cells and a group of 28 P-cells in the monkey retina. The semi-saturation contrast (S) was 0.13 for the M-cells, but 1.74 for the P-cells. This means that the contrast response of retinal M-cells was much more compressive than that of P-cells. This was also true in the few examples of ganglion cell contrast-response functions shown by Croner and Kaplan [21]. Similar evidence comes from the analysis of LGN cells by Sclar et al. [22] who fitted a slightly more complex version of Eq. (3) to their response functions. We re-plotted the LGN response functions for 2 P-cells and 2 M-cells, representing the upper and lower thirds of each population distribution. We fitted

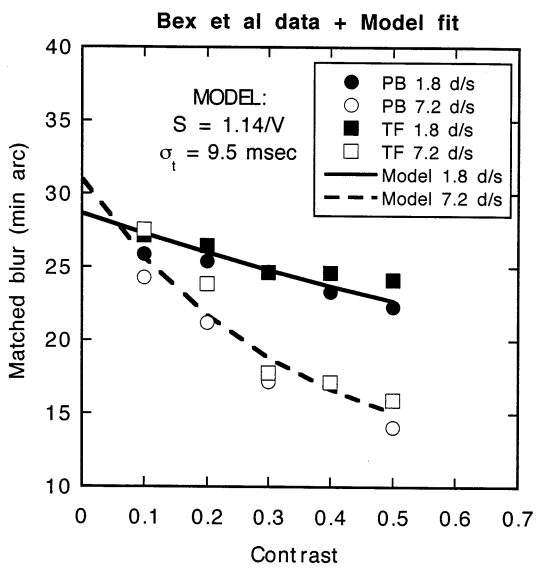

Fig. 6. The 2-parameter model fitted to the data of Bex et al. [12].

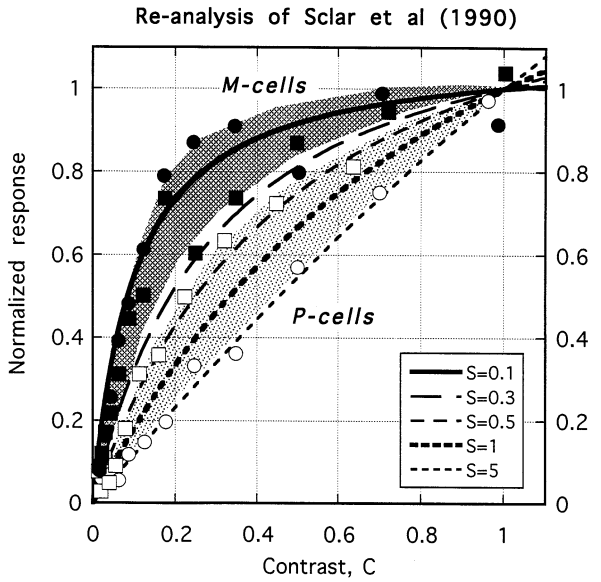

Fig. 7. Contrast response of M and P cells in the monkey LGN. Open symbols: two representative P-cells; filled symbols: two representative M-cells. Curves show how the shape of the transducer (Eq. (3)) varies with parameter S. (Data re-plotted from Sclar et al. [22] Fig. 1).

Eq. (3) and found that $S = 0.11, 0.17$ for the two M-cells, but $S = 0.48, 3.53$ for the two P-cells. We then normalized the four sets of cell data (scaled to have the same fitted value at $C = 1$) on linear axes, as shown in Fig. 7. One of the P-cells ($S = 3.53$) is nearly linear (a fact that is obscured on a log contrast axis) while the other is moderately compressive ($S = 0.48$). Both M-cells are more compressive than the P-cells. The heavy curves in Fig. 7 are based on Sclar et al.'s median values and represent a guess at the response functions that might best represent the LGN P ($S = 1$) and M ($S = 0.1$) populations as a whole. These curves are very close to the mean curves plotted by Kaplan et. al. [21] for retinal P-cells and M-cells ($S = 1.74$ and $S = 0.13$, respectively).

We can now compare these physiological values of S with those derived from the blur-matching data. For observer SH, $S = 1.59/V$, and so at $16°s^{-1}$ $S = 0.1$, while at $1.6°s^{-1}$ $S = 1.0$. This suggests that at high speeds perceived blur is mediated by mechanisms whose contrast response is similar to M-cells, while at low speeds the contrast response is similar to that of P-cells. At intermediate speeds perceived blur presumably reflects a changing mixture of P-like and M-like contributions, with the balance weighing more heavily towards M as speed increases. This proposal requires the balance of responding between P and M to vary smoothly with speed, such that the effective value of S is inversely proportional to V. This is plausible, since the relative sensitivity of P and M pathways seems to vary directly with speed. Merigan and Eskin [23] found that when the P-cell pathway was selectively damaged by a neurotoxin, the consequent loss of behavioural

contrast sensitivity varied with both spatial and temporal frequency of the test grating but seemed to depend most directly on speed-the ratio of temporal to spatial frequencies. Sensitivity loss was greatest at low speeds and least at high speeds. Conversely, magno-cellular (M) lesions produced loss of contrast sensitivity at high speeds, not low [24]. These complementary findings are consistent with the idea that in responding to a moving stimulus the relative contributions of P and M populations vary directly with speed.

Our suggestion, then, is that ganglion cells and LGN cells vary in their degree of local contrast compression, and that the more compressive cells are increasingly recruited as speed increases. An alternative implementation might be that the compressiveness of individual cells varies with speed, through some dynamic property or adaptive effect. We have no evidence to support this view at present, and so favour the P/M interpretation because it is reasonably well supported by neurophysiological and neurobiological evidence. We emphasize, though, that the computational analysis given here holds good, no matter which implementation may be favoured.

Very recently, Galvin et. al. [25] reported that blurred edges in peripheral vision (up to 40° eccentricity) appeared considerably sharper than those in foveal vision, while sharp peripheral edges looked more blurred than in the fovea. The analogy with our results is striking, and suggests that peripheral viewing and high image speed affect edge sharpness via a common mechanism. The idea that this common mechanism is the M-cell pathway is further strengthened by Dacey's [26] finding that in human retina the proportion of ganglion cells that are of the parasol type (M-cells) increases greatly with eccentricity. Thus with increasing eccentricity or speed the encoding of edge sharpness may increasingly be carried by the M-cell population.

In summary, we have shown that a model with two main factors accounts well for the perception of blur during motion. The two free parameters of the model, σ_t and α, are consistent with previous psychophysical and physiological estimates of the S.D. of the temporal impulse response and semi-saturation constant of primate M and P cells respectively. Moreover, the model is qualitatively consistent with the results of Hammett and Bex [13]. They found that adaptation to a missing-fundamental pattern attenuated motion sharpening, and suggested that sharpening may be due to a non-linearity which serves to introduce high spatial frequencies into the effective neural image that are not present in the retinal image. We propose here that the most likely candidate for such a mechanism is the early local contrast non-linearity which forms the second stage of the present model. No special motion de-blurring process seems to be required.

Anderson [27] has reported distortions in the perceived profile of complex moving waveforms which may be explained by phase shifts of the higher harmonics. His findings show that spatial frequency dependent temporal delays can distort moving waveforms. But temporal delays cannot easily account for motion sharpening since sinusoidal gratings are equally susceptible to motion sharpening. No higher harmonics are present in these gratings, and so even with a delay they would remain sinusoidal. In the absence of non-linearity, temporal delay could not account for their enhanced sharpness.

We conclude that moving edges are blurred by temporal integration over an interval of about 20 ms, and sharpened by the compressive response of visual mechanisms to the local contrast values in the spatial waveform. The degree of compression increases smoothly with increasing speed, and this speed-dependent transduction accounts for the effects of both contrast and speed on perceived blur, over a 50-fold range of blurs. We suggest that the most plausible physiological implementation of these two stages is an early (photoreceptoral) temporal filtering stage followed by a stage which encodes local contrast in a speed-dependent manner, perhaps due to differential recruitment of M and P cells.

Acknowledgements

We express our thanks to two anonymous referees for many valuable suggestions on an earlier draft of this paper. ST Hammett was supported by the Wellcome Trust, MA Georgeson was supported by the BBSRC (Grant S03969) and A Gorea was supported by Grant 95-1195/A000/DRET/DS/SR.

References

[1] Gorea A, Tyler CW. New look at Bloch's law for contrast. J Opt Soc Am A 1986;3:52–61.
[2] Georgeson MA. Temporal properties of spatial contrast vision. Vis Res 1987;25:765–80.
[3] Barlow HB. Temporal and spatial summation in human vision at different background intensities. J Physiol 1958;141:337–50.
[4] Legge GE. Sustained and transient mechanisms in human vision: temporal and spatial properties. Vis Res 1978;18:69–81.
[5] Chen S, Bedell HE, Ögmen H. A target in real motion appears blurred in the absence of other proximal moving targets. Vis Res 1995;35:3215–328.
[6] Pääkkönen AK, Morgan MJ. Effects of motion on blur discrimination. J Opt Soc Am A 1994;11:992–1002.
[7] Hammett ST. Motion blur and motion sharpening in the human visual system. Vis Res 1997;37:2505–10.
[8] Burr DC. Motion smear. Nature 1980;284:164–5.
[9] Burr DC, Ross J, Morrone MC. Seeing objects in motion. Proc R Soc London B Biol Sci 1986;227:249–65.

[10] Anderson CH, Van Essen DC. Shifter circuits: a computational strategy for dynamic aspects of visual processing. Proc Natl Acad Sci USA 1987;84:6297–301.
[11] Martin KE, Marshall JA. Unsmearing visual motion: development of long range horizontal intrinsic connections. In: Hanson SJ, Cowan JD, Giles CL, editors. Advances in neural information processing systems, vol. 5. San Mateo, CA: Morgan Kauffman, 1993.
[12] Bex PJ, Edgar GK, Smith AT. Sharpening of drifting, blurred images. Vis Res 1995;35:2359–546.
[13] Hammett ST, Bex PJ. Motion Sharpening: evidence for the addition of high spatial frequencies to the efffective neural image. Vis Res 1996;36:2729–33.
[14] Ramachandran VS, Madhusudhan Rao V, Vidyasgar TR. Sharpness constancy during movement perception. Perception 1974;3:97–8.
[15] Ögmen H. A neural theory of retino-cortical dynamics. Neural Networks 1993;6:245–73.
[16] Taylor MM, Creelman CD. PEST: Efficient estimates on probability functions. J Acoust Soc Am 1967;41:782–7.
[17] Georgeson MA. From filters to features: location, orientation, contrast and blur. In: Ciba Foundation Symposium, 184. Higher Order Processing in the Visual System. New York: Wiley, 1994.
[18] Bracewell RN. The Fourier transform and its applications. New York: McGraw-Hill, 1986.
[19] McKee SP, Taylor DG. Discrimination of time: comparison of foveal and peripheral sensitivity. J. Opt. Soc. Am. 1984;1:620–7.
[20] Watson AB. Derivation of the impulse response: Comments on the method of Roufs and Blommaert. Vis Res 1982;22:1335–7.
[21] Kaplan E, Lee BB, Shapley RM. New views of primate retinal function. In: Osborne NN, Chader GJ, (editors). Progess in Retinal Research, 1990;9:273–336.
[22] Sclar G, Maunsell JHR, Lennie P. Coding of image contrast in central visual pathways of the macaque monkey. Vis Res 1990;30:1–10.
[23] Merigan WH, Eskin TA. Spatio-temporal vision of macaques with severe loss of Pβ retinal ganglion cells. Vis Res 1986;26:1751–61.
[24] Merigan WH, Byrne CE, Maunsell JHR. Does primate motion perception depend on the magnocellular pathway? J Neurosci 1991;11:3422–9.
[25] Galvin SJ, O'Shea RP, Squire AM, Govan DG. Sharpness overconstancy in peripheral vision. Vis Res 1997;37:2035–9.
[26] Dacey DM. Physiology, morphology and spatial densities of identified ganglion cell types in primate retina. In: Ciba Foundation Symposium 184. Higher-order processing in the visual system. New York: Wiley, 1994; 12–28.
[27] Anderson SJ. Visual processing delays alter the perceived spatial form of moving gratings. Vis Res 1993;33:2733–46.